Comparative study of wheat low-molecular-weight glutenin and alpha-gliadin trafficking in tobacco cells

Mathilde Francin-Allami, Axelle Bouder, Yves Popineau

Comparative study of wheat low-molecular-weight glutenin and α-gliadin trafficking in tobacco cells.

Mathilde Francin-Allami*, Axelle Bouder, Yves Popineau.

INRA, UR1268, Biopolymères Interactions Assemblages, 44300 Nantes, France

***Corresponding author**

E-mail: allami@nantes.inra.fr

Abstract

Wheat prolamins are the major proteins that accumulate in endosperm cells and are largely responsible for the unique biochemical properties of wheat products. They are accumulated in the endoplasmic reticulum (ER) where they form protein bodies (PBs) and are then transported to the storage vacuole where they form a protein matrix in the ripe seeds. Whereas previous studies have been carried out to determine the atypical trafficking pathway of prolamins, the mechanisms leading to ER retention and PB formation are still not clear. In this study, we examined the trafficking of a low-molecular-weight glutenin subunit (LMW-glutenin) and α-gliadin fused to fluorescent proteins expressed in tobacco cells. Through transient transformation in epidermal tobacco leaves, we demonstrated that both LMW-glutenin and α-gliadin were retained in the ER and formed mobile protein body-like structures (PBLS) that generally do not co-localise with Golgi bodies. An increased expression level of BiP in tobacco cells transformed with α-gliadin or LMW-glutenin was observed, suggesting the participation of this chaperone protein in the accumulation of wheat prolamins in tobacco cells. When stably expressed in BY-2 cells, LMW-glutenin fusion was retained longer in the ER before being exported to and degraded in the vacuole, compared to α-gliadin fusion, suggesting the involvement of intermolecular disulphide bonds in ER retention, but not in PBLS formation. Co-localisation experiments showed that gliadins and LMW-glutenin were found in the same PBLS with no particular distribution, which could be due to their ability to interact with each other as indicated by yeast two-hybrid assays.

Keywords

Wheat - Gliadin - Low-Molecular-Weight Glutenin - Tobacco cells - Trafficking - Fluorescent proteins

Key message

Wheat low-molecular-weight-glutenin and α-gliadin were accumulated in the endoplasmic reticulum and formed protein body-like structures in tobacco cells, with the participation of BiP chaperone. Possible interactions between these prolamins were investigated.

Abbreviations:

BiP: Binding protein

BY-2:	Bright Yellow-2
ER:	Endoplasmic reticulum
GFP:	Green fluorescent protein
HMW:	High molecular weight
HMW-G:	High-molecular-weight glutenin
LMW:	Low molecular weight
LMW-G:	Low-molecular-weight glutenin
$mRFP_1$:	Monomeric red fluorescent protein
PDI:	Protein disulphide isomerase
PBLS:	Protein body-like structure
PB:	Protein body

Introduction

Wheat is the most widely cultivated cereal and the most widely consumed food crop in the world. Wheat seed storage proteins, prolamins, are the major components that accumulate in wheat endosperm cells, and are largely responsible for the viscoelasticity properties of gluten. Prolamins are divided into two fractions, glutenins and gliadins, according to their polymerisation state. Glutenins are polymers that have intra- and interchain disulphide bonds composed of low-molecular-weight and high-molecular-weight glutenin subunits (LMW-G and HMW-G, respectively) (Payne 1987). Gliadins are monomers with intramolecular disulphide bonds (α and γ-gliadins) or without disulphide bonds (ω-gliadins) (Bietz et al. 1977). Gliadins account for about 40-50% of the total proteins in wheat seeds and play an important role in the nutritional and processing quality of flour. γ-gliadins have been considered to be the oldest proteins in the wheat prolamin family. HMW-glutenin subunits are composed of a central repetitive domain flanked by two non-repetitive regions containing cysteine residues critical for glutenin cross-linking. LMW-glutenin subunits are structurally related to monomeric α and γ-gliadins except that they contain two additional cysteine residues available for interchain disulphide formation, which would be responsible for the polymeric feature of these proteins (Shewry and Tatham 1997).

In seed endosperm cells, prolamins are synthesized in the endoplasmic reticulum (ER), where they accumulate. They form storage structures known as protein bodies (PBs) in the ER, and are then transported to the storage vacuole (Parker and Hawes 1982; Levanony et al. 1992; Altschuler et al. 1993; Galili et al. 1993). It seems that the major part of prolamins are transported from the ER to the storage vacuole, bypassing the Golgi, via the PBs in endosperm cells (Levanony et al. 1992; Galili et al. 1993; Hara-Nishimura et al. 1998; Vitale and Galili 2001). Prolamins were also recently found to accumulate in maize aleurone cells in a similar Golgi-independent pathway (Reyes et al. 2011). However, prolamins were also detected in the Golgi stacks, especially during the early stage of seed development (Parker and Hawes 1982; Galili et al. 1993; Shy et al. 2001; Loussert et al. 2008; Tosi et al. 2009).

PBs disappear during seed maturation to form the protein matrix around the starch granules (Rubin et al. 1992). In wheat seeds, the distribution of the different prolamins within the protein bodies is still unclear. No particular spatial organisation of gliadins and glutenins has been observed in wheat PBs (Loussert et al. 2008), contrary to the prolamins found in maize (Coleman et al. 1996, 2004) and rice PBs (Nagamine et al. 2011). However, a segregation of

protein type into a specific population of protein bodies can occur within the same endosperm cell (Tosi et al. 2009). A segregation of gluten proteins occurred both between and within the protein bodies during protein deposition. A recent study indicated that differential patterns of distribution were found for the HMW glutenin subunits and γ-gliadin (more abundant in the inner endosperm layers) when compared to the LMW-G and other gliadins (ω and α-gliadins were more abundant in the subaleurone) (Tosi et al. 2011).

The mechanisms leading to the trafficking and accumulation of prolamins during seed development are only partially known. Indeed, prolamins do not contain the classical ER retention signals such as HDEL/KDEL, and the process leading to their retention in the ER is not known. Several mechanisms have been suggested, including the involvement of the repeated motif of prolamins for ER retention, as demonstrated for wheat gliadins expressed in yeast (Rosenberg et al. 1993), xenopus oocytes (Altschuler et al. 1993) and, more recently, in *Nicotiana tabacum* leaves (Francin-Allami et al. 2011). These repeated motifs could be used as an anchor for the interaction of prolamins to the ER membrane, which would explain their retention in the ER (Banc et al. 2009). However, the repeated sequence was not the only one to contribute to the accumulation of prolamins in the ER and PBs. Disulphide bonds could also play an essential role in ER retention and the accumulation of wheat prolamins (Shimoni and Galili 1996; Lombardi et al. 2009). More recently, it was proposed that both cysteine-rich C-terminal and repeated N-terminal domains of γ-gliadin were involved in γ-gliadin ER retention and protein body-like structure formation (Francin-Allami et al. 2011). The participation of chaperone proteins and, in particular, the ER luminal BiP, was also demonstrated (Levanony et al. 1992; Li et al. 1993; Muench et al. 1997; Saito et al. 2009). In rice, it has been suggested that BiP is necessary to maintain prolamins in a competent state for subsequent assembly in the ER (Muench et al. 1997). It has also been suggested that the disulphide isomerase (PDI) participates in the segregation of rice prolamins within the ER lumen (Takemoto et al. 2002).

Trafficking of a wheat γ-gliadin and HMW-G subunit fused to a fluorescent protein was recently investigated, demonstrating that tobacco cells are a good model for studying atypical wheat prolamin trafficking (Francin-Allami et al. 2011; Saumonneau et al. 2011). In order to further elucidate the trafficking pathway of wheat seed storage prolamins, we decided to study other typical wheat prolamin components such as a LMW-G subunit and an α-gliadin, which account for the majority of the storage proteins in the endosperm. To do this, we used a fluorescent protein fusion strategy and a tobacco cell model. The results indicated that the two

prolamins were accumulated in the ER network and were able to form numerous protein body-like structures in tobacco cells. We also investigated the potentiality of interactions between the different prolamins. Taken together, these results provide global information concerning the trafficking and assembly of wheat seed storage proteins.

Materials and methods

Plasmid constructs

Gateway system cloning was used to perform the different constructs used in this study, according to the manufacturer's instructions (Invitrogen). The binary vectors pMDC83 (Curtis and Grossniklaus 2003) and pK7RWG2 (Karimi et al. 2005) were used to construct C-terminal GFP/mRFP$_1$ fusions with the different wheat ("Recital" variety) prolamin cDNAs. The cDNA encoding α-gliadin (see nucleotide and amino acid sequences in supplementary Fig. S1) was amplified using the primers AttB1-A4-PS (5'-aaa aaa gca ggc ggc ttc atg aag acc ttt ctc atc) and AttB2-A4 (5'-caa gaa agc tgg gtc gtt agt acc gaa gat), followed by a second PCR with the primers AttB1 (5'-ggg gac aag aag aag ttt gta caa aaa agc agg ct) and AttB2 (5'-ggg gac cac ttt gta caa gaa agc tgg gt). The cDNA encoding the low molecular weight glutenin (LMW-G) (see nucleotide and amino acid sequences in supplementary Fig. S2) was amplified using the primers AttB1-LMWG-PS (5'-aaa aaa gca ggc ttc atg aag acc ttc ctc) and AttB2-LMWG (5'-caa gaa agc tgg gtc gta ggc acc aac tcc ggt), followed by a second PCR with the primers AttB1 and AttB2.

The constructs of γ-gliadin in fusion with GFP and mRFP$_1$ were previously described in Francin-Allami et al. (2011).

In order to perform yeast two-hybrid experiments, the cDNAs encoding the α-gliadin and LMW-G were cloned into pACT2 prey and pAS2-1 bait vectors (Clontech). The cDNAs were amplified using the primers A4NcoIVRV-5' (5'-c cat gcc atg gca gtt aga gtt cca gtg cca caa ttg-3') and A4BamHI-3' (5'-cg gga tcc tca gtt agt acc gaa gat gcc aaa tgg-3') for α-gliadin amplification, and the primers L3NcoI-5' (5'-c cat gcc atg gca cag atg gag act aga tgc atc cct-3') and L3BamHI-3' (5'-cg gga tcc tca gta ggc acc aac tcc ggt-3') for LMW-G amplification. γ-gliadin cDNA was cloned into pAS2-1 vectors using the primers Gb5ncoI-NIQ-5' (5'-c cat gcc atg gca aat ata cag gtc gac cct agc ggc-3') and Gb5bamHI-3' (5'-cg gga tcc tca ttg gcc acc aat gcc ggc-3'). NcoI and BamHI were used as restriction sites.

Transient expression in plants

Transient expression in tobacco leaf epidermal cells was performed as described by Sparkes et al. (2006). *Nicotiana tabacum* plants were grown in a growth chamber under a 16 h

photoperiod control at 21°C for 5-6 weeks prior to Agrobacterium infiltration. The recombinant binary vectors were transferred into *Agrobacterium tumefasciens* (strain GV3101::mp90) by heat shock transformation. Transformed Agrobacteria were inoculated in a Luria-Bertani (LB) medium supplemented with the appropriate antibiotics at 28°C overnight. Cultures were then centrifuged and washed with infiltration buffer (5 g l^{-1} glucose, 50 mM MES, 2 mM $Na_3PO_4.12H_2O$, 100 µM acetosyringone) before being resuspended with this same buffer at a DO600nm=0.1 and 0.05 for prolamin constructs and marker vectors (ER and Golgi), respectively. The diluted bacteria were delivered to lower leaves of *N. tabacum* by gentle pressure infiltration using a syringe. For experiments using co-expression, bacteria containing the constructs were mixed in appropriate volumes before performing the infiltration.

Stable transformation of BY-2 suspension cells

Suspension-cultured tobacco cells (BY-2, Bright Yellow 2) were provided by Chris Hawes (Oxford Brookes University, UK), and cultured at 24°C in the dark in a Murashige and Skoog-MES medium (Duchefa, no. MO254) supplemented with 20 mg l^{-1} KH2PO4, 100 mg l^{-1} myo-inositol, 30 g l^{-1} sucrose, 1 mg l^{-1} thiamine and 0.2 mg l^{-1} 2.4 D, pH 5.6. The binary gateway-plasmid constructs were transferred into the GV3101::mp90 *Agrobacterium tumefaciens* strain by heat shock. Transformed Agrobacteria were selected in LB medium supplemented with appropriate antibiotics and were used to transform BY-2 cells as described by Gomord et al. (1998). The transformed BY-2 calli were then screened by fluorescent microscopy and selected calli were used to initiate transgenic suspension cell cultures. One ml of cells was transferred to a fresh 30 ml of medium every week.

To compare the growth rate curves in the different BY-2 lines, the cells were filtered each day from independent Erlenmeyer flasks on a 0.45 µm Millipore filter, and the fresh cell weight determined.

Confocal laser scanning microscopy

Confocal microscopy experiments were performed at the Biopolymers-Structural Biology platform, INRA Nantes (France). An inverted Nikon A1 confocal laser scanning microscope was used to examine the subcellular localisation of GFP and $mRFP_1$ fluorescence. The samples were examined with a water-immersion X40 objective. GFP and mRFP channels

were acquired by alternately scanning with line switching, using a 488 nm argon laser line for excitation of the GFP and a 561 nm laser line for $mRFP_1$: emissions were collected via a photomultiplier through a 515+/-30 nm and a 595+/-50 nm band-pass filters, with the same gain settings for every experiments. Images were processed using NIS-Element (Nikon) and Image J software.

Transmission electron microscopy

Infiltrated leaves were cut in 1 mm^3 samples and placed in a fixation solution consisting of 2% (w/v) paraformaldehyde and 2.5% (v/v) glutaraldehyde in 0.1M phosphate buffer (pH 7.2). Air was removed from leaf samples with air vacuum cycles. Samples were then fixed at 4°C in the fixation solution overnight. Fixed samples were rinsed in phosphate buffer and de-ionised water prior to postfixation with 1% osmium tetraoxide during 1 hour. Dehydration was performed in 30, 50, 70, 85, 95 and 100% ethanol solutions. Samples were successively impregnated with 50/50 and 0/100 ethanol/propylene oxide (v/v) for 1 hour, then 50/50 propylene oxide/Epon (Epoxy Embedding Medium Kit, 45359-1EAF Sigma Aldrich) (v/v) 1 hour and 0/100 overnight. The impregnated samples were polymerised for 24 h at 55°C and 60 h at 72°C. A Leica EM UC7 Ultramicrotome (Leica) was used for making ultrathin sections (80 nm) for electron microscopy. Sections were collected on copper grids, counterstained with 2% uranyl acetate and examined on a JEOL 1230 TEM (JEOL; accelerating voltage of 80 kV).

Treatments with Latrunculin B inhibitor

Tobacco leaf sections were incubated for 40 min in a 25-µM solution of Latrunculin B (Calbiochem). Treated cells were then visualised by confocal microscopy. Each treatment with inhibitor was repeated at least twice with similar results.

Protein extraction and immunoblot analysis

Tobacco BY-2 cells were harvested by filtration and resuspended in a SDS sample buffer (100 mM TRIS-HCL, pH 6.8, 4% SDS, 20% glycerol, 5% 2-mercaptoethanol, 100 µg ml^{-1} bromophenol blue) prior to boiling for 5 min, and then centrifuged. The supernatant was subjected to SDS-PAGE according to Laemmli (Laemmli, 1970) with a separating gel

containing 4-20% acrylamide in gradient (mini-PROTEAN TGX gels, Biorad). Each protein extract loaded on the gel corresponded to the same volume of filtered cells.

Infiltrated tobacco leaf sections were cut, crushed in liquid nitrogen, rinsed in acetone, and dried. The leaf powders were weighed and an equal amount of powders was resuspended in SDS sample buffer. 15 mg of leaf extracts were loaded to the each lanes of gel for immunoblotting.

Proteins were then electrotransferred to a nitrocellulose membrane (IBlot Gel Transfer Stacks Nitrocellulose, Invitrogen) before immunodetection by specific antibodies. Immunoblotting was performed using mouse monoclonal anti-GFP antibodies (dilution: 1:2500) (Clontech), or rabbit polyclonal anti-BiP antibodies (dilution: 1:4000) (Hatano et al. 1997). An alkaline phosphatase-conjugated goat anti-mouse (dilution: 1:2000) or anti-rabbit (dilution: 1:3000), respectively, were used for the detection. Proteins were stained with BCIP-NBT (Promega kit) according to the manufacturer's instructions.

Yeast two-hybrid assays

Yeast two-hybrid assays were performed in *Saccharomyces cerevisiae* strain Y190 (*MATa, gal4, gal80, his3, trp1, ade2, ura3, leu2, URA3::GAL1::lacZ, LYS2::GAL4(UAS)::HIS3 cyh*^{R}). Y190 was transformed with a pair of plasmids expressing Gal4BD fusion TRP1 (bait) and Gal4AD fusion LEU2 (prey), plated onto selected media (YNBD medium (0.17% yeast nitrogen base without amino acids, 2% glucose, 2% agar) supplemented with appropriate amino acids and bases) for 4-5 days at 28°C, and tested for β-galactosidase production in an overlay plate assay.

Results

Prolamin constructs

Wheat α-gliadin has two main domains: a repeated N-terminal domain rich in glutamine and proline residues, and a C-terminal domain containing six cysteines to form intramolecular bonds. LMW-G has three domains: one repeated domain rich in glutamine and proline surrounded by a small non-repeated domain with one cysteine at the N-terminal extremity, and a larger non-repeated domain containing seven cysteines at the C-terminal extremity (Fig. 1). Both α-gliadin and LMW-G have a signal peptide that is cleaved off during protein synthesis. In order to investigate the trafficking of wheat α-gliadin and LMW-G, the corresponding genes were isolated from wheat endosperm cDNA at 250 degree days after anthesis. They were then cloned into binary vectors containing a double 35S promoter of cauliflower mosaic virus and the enhanced green fluorescent protein (eGFP) or monomeric red fluorescent protein ($mRFP_1$) coding sequences downstream from the gateway cassette, leading to a C-terminal GFP/$mRFP_1$ fusion of the prolamins (Fig. 1). These constructs were used to transform tobacco leaf epidermal cells and BY-2 suspension cultured cells in order to study the subcellular localisation of α-gliadin and LMW-G.

Gliadin and glutenin localisation in tobacco cells

The subcellular localisation of α-gliadin and LMW-G was first investigated after transient transformation in epidermal tobacco leaf cells via Agrobacterium infiltration. Cells expressing the α-gliadin fused to GFP presented fluorescence in the ER compartment, which was confirmed by the co-localisation with an ER marker ($mRFP_1$-DPL1; Marion et al. 2008; Tsegaye et al. 2007) (Fig. 2a, b). The fluorescence observed by confocal microscopy was mainly represented by punctate structures instead of a typical ER network. These punctate structures have already been described for γ-gliadin transformed tobacco leaves where they were identified as protein body-like structures (PBLS) (Francin-Allami et al. 2011). α-gliadin PBLS often form clusters that look like bunches of grapes, leading to large aggregated structures. We also fused LMW-G with green fluorescent protein and used it to transiently transform tobacco leaf cells. The observation of fluorescence by confocal microscopy

indicated that LMW-G was also expressed in ER and forms large PBLS (> 4 µm in diameter), which tended to group together to form clusters (Figs. 2d, e). Like those formed by the expression of gliadin, these PBLS seemed to be surrounded by the ER marker DPL1, which is an ER membrane lyase, indicating that ER membranes encapsulate the bodies (Fig. 2e, high magnification of the inset). α-gliadin and LMW-G seemed to be able to form more systematically and well-defined PBLS compared to those previously obtained with γ-gliadin constructs. Moreover, quantitative data indicated that whereas α-gliadin was accumulated as numerous and relatively small PBLS, LMW-G formed less numerous but often larger PBLS (Fig. 3). Western blot analysis of leaf cells expressing α-gliadin-GFP and LMW-G-GFP with anti-GFP antibodies confirmed the integrity of the fused proteins, with an apparent molecular mass of approximately 70 kDa (Fig. 4a). A fragment of lower mobility was also present at a very low level, and corresponded to the mass of free GFP (27 kDa).

α-gliadin and LMW-G PBLS are highly mobile, and we demonstrated using Latrunculin treatment that this mobility is actin-dependent (see movies S3 and S4 in supplementary data). Because PBLS are very mobile and similar to Golgi bodies, we tested the co-localisation with the Golgi marker, ST-RFP (sialyl transferase signal anchor-mRFP$_1$). As previously seen for γ-gliadin-GFP, the result indicated that α-gliadin and LMW-G PBLS generally did not appear to be co-localised with Golgi bodies (Figs. 2c, f), which was confirmed by a different pattern of movement of PBLS and Golgi bodies when time-lapse series of confocal images were analysed (see movie S3 in supplementary data).

PBLS morphology

In order to reveal the morphology of the gliadins and glutenin PBLS, the transformed tobacco leaves were submitted to appropriate treatment (see the Materials and Methods section), and examined by electron microscopy. The focalisation on the ER region of tobacco cells showed relatively round shape structures next to conventional tubular ER when cells expressed α-gliadin or LMW-G (Figs. 5a, b). These structures reflected the PBLS structures observed with confocal microscopy. The PBLS structures were not seen to be continuous with the ER in these images. It is however not excluded that PBLS were still linked to the ER network, or in contrary they bud off the ER and localized in the cytosol. Their size (< 1µm) corresponded to the smallest PBLS observed with fluorescent microscopy. This was consistent with previously

studies describing PBLS formed in tobacco leaves after expression of maize β-zein (Randall et al. 2005) or wheat γ-gliadin (Francin-Allami et al. 2011).

Gliadin and LMW-glutenin are degraded in the vacuole of BY-2 cells

In order to examine the dynamic trafficking of prolamins in a stable system, we expressed α-gliadin and LMW-G fused to GFP in BY-2 suspension cultured cells. As previously seen after transient infiltration in tobacco leaves, α-gliadin and LMW-G were localised in the ER network (Fig. 6a). Numerous and well-defined PBLS were formed with both prolamins. Quantitative data indicated that both prolamins could form PBLS with a diameter larger than 1 µm, and that α-gliadin tended to include more cells with numerous and larger PBLS than cells expressing LMW-G (Fig. 3). After 2-4 days of subculturing, no fluorescence was seen in the vacuole (Table 1). After four days of subculturing, in addition to the ER and PBLS, fluorescence was also seen in the vacuole of the α-gliadin transformed cells. At 7 days of subculturing, almost all of the fluorescence was localised in the vacuole. These results were in accordance with the changes previously observed in the case of γ-gliadin, where fluorescence in the vacuole corresponded to the release of GFP core after transport of γ-gliadin-GFP to the vacuole (Francin-Allami et al. 2011). In LMW-G expressing cells, fluorescence was also clearly detected in the ER with the formation of numerous PBLS. The release of fluorescence into the vacuole was slower since no or little fluorescence was observed in the vacuole of cells at 7 days after subculturing, and even at 10 days after subculturing, there was still fluorescence in the ER network in addition to the vacuole (Fig. 6a, Table 1). These results were confirmed by immunoblotting analysis where LMW-G-GFP was still detected at 10 days after subculturing, whereas only GFP is detected in the cells expressing α-gliadin as early as 7 days of subculturing (Figs. 7a, b). It is noteworthy that no cell growth difference was detected between the two lines expressing α-gliadin or LMW-G (supplementary Fig. S5). The same pattern of degradation was obtained for α- and γ-gliadin-GFP, whereas LMW-G showed a slower degradation than gliadins. It is also interesting to note that the amount of PBLS decreased with the stage of cell development for both transformed BY-2 cell lines (Table 1). Whereas α-gliadin-GFP transformed cells tended to have more PBLS at 5-7 days of subculturing but with rapid degradation in the vacuole, LMW-G-GFP transformed cells presented a fluorescence mainly localised in the ER network with less PBLS at these stages (Table 1, Fig. 6).

BiP expression in transformed tobacco cells

Because BiP is a typical ER-resident protein, and some studies have indicated that it is involved in the folding and assembly of proteins in the ER, we decided to follow the expression of this chaperone protein during the expression of gliadin and glutenin in tobacco cells. Immunoblotting indicated an increased expression of BiP in epidermal tobacco cells infiltrated with α-gliadin-GFP or LMW-G-GFP compared to the non-transformed plant (Fig. 4b). In the same way, expression of BiP is increased in the BY-2 suspension cultured cells stably transformed with α-gliadin and LMW-G (Figs. 7a, b). Moreover, the expression of BiP decreased as days of subculturing increased, which is in relation to the progressive degradation of fused prolamins. At 10 subculturing days of cells expressing LMW-G or 7 subculturing days of cells expressing α-gliadin, the expression level of BiP was identical to that of non-transformed BY-2. Besides, we demonstrated that the expression level of BiP was relatively constant during subculturing of non-transformed BY-2 cells (Fig. 7c). In addition, differential centrifugation indicated that a part of the BiP in BY-2 cells expressing α-gliadin-GFP at four days of subculturing was found in the vacuolar fraction (Fig. 7d). This result is consistent with those previously found (Tamura et al. 2004).

Co-localisation of prolamins in tobacco cells

The distribution of the different prolamins within the protein bodies in wheat endosperm is not really clear. To determine their distribution in PBLS, gliadins and LMW-G were co-expressed in tobacco leaf epidermal cells (Fig. 8). Confocal images indicated that γ-gliadin and α-gliadin co-localised in protein bodies. All PBLS inside the tobacco cells contained both gliadins. In the same way, we demonstrated that LMW-G was co-localised with α-gliadin or γ-gliadin in all protein bodies. In addition, at the resolution provided by confocal microscopy, all these combinations of proteins appeared to be homogeneously distributed inside PBLS. These co-localisations within PBLS lead to the possibility that prolamins could interact with each other. In order to test this possibility, a yeast two-hybrid experiment was performed using the different combinations of prolamins. A yeast two-hybrid system was previously used to detect interactions between maize prolamins (Kim et al. 2002) or wheat γ-gliadin domains (Francin-Allami et al. 2011). For this, gliadins and LMW-G genes were cloned into

specific yeast two-hybrid vectors, in order to fuse the genes at their N-terminals with the activation domain or binding domain of the yeast GAL4 transcription factor. The results indicated that all prolamins could interact with each other in an *in vitro* yeast two-hybrid system (Table 2). α-gliadin seemed to have a particularly good ability to interact with other proteins, revealed by the fact that the detected interactions were strong when one of the interacting proteins was α-gliadin. We also demonstrated that α-gliadin and LMW-G were able to interact with themselves in this yeast two-hybrid context. Negative controls were performed to check that proteins were not able to directly interact with the GAL4 activation or binding domain. Thus, interactions tested by the yeast two-hybrid system reinforced the possible interaction between gliadins and LMW-G in PBLS, as suggested by co-localisation experiments with confocal microscopy.

Discussion

We demonstrated that wheat α-gliadin and LMW-G fused to GFP are stably expressed in non-seed tissue, indicating that intrinsic molecular properties of these proteins are involved in ER retention and PBLS biogenesis. This result was also found in the case of the expression of γ-gliadin (Francin-Allami et al. 2011), HMW-glutenin (Saumonneau et al. 2011) and γ-zein (maize storage protein) (Randall et al. 2005) in tobacco leaves. In addition, ER retention of LMW-G was also demonstrated in tobacco protoplasts (Lombardi et al. 2009). Both α-gliadin and LMW-G have a repeated proline-rich N-terminal domain and a more hydrophobic disulphide-rich domain, like the majority of wheat prolamins. As previously suggested, these particular domains are both probably involved in prolamin trafficking. It has been proposed that the hydrophobicity and disulphide bond formation promote specific interactions that result in the formation of large self-assemblies that are responsible for retention in ER and PB formation (Kawagoe et al. 2005; Pompa and Vitale 2006). The isolated C-terminal domain of wheat γ-gliadin in fusion with GFP was retained and was able to form PBLS when expressed in tobacco leaves or BY-2 cells (Francin-Allami et al. 2011). Based on site-directed mutagenesis of prolamin cysteine residues, the critical role of specific cysteines for PB formation was demonstrated for maize γ-zein (Llop-Tous et al. 2010).

It has been shown that the N-terminal proline-rich repeated domain of prolamins participates in ER retention and PB formation in maize (Geli et al. 1994; Llop-Tous et al. 2010) and wheat (Francin-Allami et al. 2011), although the repeated motif sequences of γ-zein are different from those of wheat prolamins. A minimal repeated motif sequence is required for PB induction. For example, the deletion of 105 amino acids from the repeated sequence of the HMW-glutenin fused to GFP reduces the ability of the glutenin to form PBLS in the ER (Saumonneau et al. 2011). The ability of a hydrophobic elastin-like protein (ELP) fusion to induce PB formation in plant leaves was recently shown, indicating the generally powerful impact of repeated motif sequences on PB formation for heterologous expression (Conley et al. 2009; Saumonneau et al. 2011).

In contrast to gliadins, glutenins form intermolecular disulphide bonds. The LMW-G sequence is very similar to monomeric α and γ-gliadins, except that it contains two additional cysteine residues available for interchain disulphide formation. In tobacco cells, gliadin and glutenin can be retained in the ER and form PBLS. However, we showed that LMW-G-GFP

was less extensively and more slowly degraded when expressed in BY-2 cells. This could be linked to the presence of these two supplementary cysteine residues and the possibility of LMW-G to form intermolecular bonds. It was previously shown that a fusion between the *Phaseolus vulgaris* vacuolar storage protein, phaseolin, and the N-terminal half of the *Zea mays* prolamin, γ-zein, forms interchain disulphide bonds that facilitate the formation of ER-located protein bodies (Pompa and Vitale 2006). Regarding the transient expression in tobacco leaves or stable transformation of BY-2 suspension cells, the quantitative data do not make it possible to distinguish a significant difference in PBLS formation between α-gliadin and LMW-G. However, we noted that in BY-2 cells, the amount of PBLS tends to decrease with the age of subculturing. Although α-gliadin was more rapidly degraded with the release of GFP in the vacuole, more PBLS were observed at the exponential phase growth compared to the LMW-G-GFP expressing cells, where fluorescence was preferentially in the ER network. Although it seems difficult to directly link the quantity of PBLS to the degradation of prolamins and the release of GFP in the vacuole, this result suggested that aggregated prolamins in PBLS could be more easily degraded in the vacuole than prolamins localised in the ER network, but this remains to be proven.

In wheat endosperm, prolamins are expressed in abundance. Protein concentration may play an important role in prolamin accumulation and PB formation. This is probably the reason why zein-GFP expressed in tobacco was not assembled into stable PBs, whereas when it was expressed in a higher concentration, it was stably retained in the ER and forms PBs (Foresti et al. 2008; Llop-Tous et al. 2010). In this case, a double 35S promoter was used to allow a high expression of α-gliadin or LMW-G in tobacco cells in order to mimic the strong expression of prolamin in wheat endosperm cells.

Molecular chaperones such as BiP and PDI are involved in ER quality control, and are known to increase in cells under ER stress (Vitale and Ceriotti 2004). Several studies have demonstrated that BiPs are involved during storage protein synthesis and stress response (Hatano et al. 1997; Muench et al. 1997; Takaiwa et al. 2009). In addition to the intrinsic prolamin properties and their expression level, molecular chaperones could play an important role in ER retention and PB formation (Levanony et al. 1992; Muench et al. 1997; Saito et al. 2009). It was suggested that the interaction of the ER luminal BiP with zein proteins could contribute to their stability and the ability to form protein bodies (Randall et al. 2005). In our study, immunoblotting revealed an increase of the BiP expression level in tobacco cells

570 transformed with α-gliadin or LMW-G, compared to the basal BiP expression level of non-
571 transformed cells. Therefore, as previously reported, BiP seems to participate in the
572 accumulation of prolamins in the heterologous tobacco cells. In addition to assist in protein
573 folding, BiP participates in the protein degradation process known as ER-associated
574 degradation (ERAD). In this case, BiP expression decreased according to the days of
575 subculturing in transformed BY-2, which is concomitant to the degradation of the prolamin
576 fusions. Differential centrifugation indicated that a part of the BiP in BY-2 cells expressing α-
577 gliadin-GFP was found in the vacuolar fraction. These results imply that BiP could contribute
578 to the degradation process of α-gliadin or LMW-G-GFP constructs and their transport to the
579 vacuole of tobacco cells, as previously demonstrated for other ER-resident protein
580 degradation (Tamura et al. 2004; Pimpl et al. 2006). Further experiments would have to be
581 carried out to determine the role of BiP and other folding proteins such as PDI on the
582 retention and accumulation of prolamins. Moreover, it was demonstrated that ER protein
583 aggregates expressed in transgenic cultured cells are degraded by autophagy when cells reach
584 the stationary phase (Tamura et al. 2004; Toyooka et al. 2006). The degradation of α-gliadin
585 or LMW-G in BY-2 cells could also be the result of an autophagy mechanism. However,
586 neither ERAD nor autophagy processes involved traffic through the Golgi apparatus, in
587 contrast with the observation made in this study for the degradation of α-gliadin-GFP and
588 LMW-G-GFP in BY-2 cells. The processing of α-gliadin-GFP and LMW-G-GFP could
589 involve an alternative pathway of vacuolar delivery via a Golgi-dependent transport, which
590 also implies the BiP chaperone (Frigerio et al. 2001; Pimpl et al. 2006).
591
592 Through the co-localisation experiment, we demonstrated that α-gliadin and LMW-G were
593 found in the same PBLS after transient infiltration in epidermal tobacco cells, and seemed to
594 be homogeneously distributed in these protein bodies. This was consistent with results
595 previously reported in wheat seed by immunostaining (Loussert et al. 2008; Tosi et al. 2009).
596 However, this does not exclude the possibility that differential patterns of distribution of the
597 seed storage prolamins exist in endogenous wheat endosperm tissue, as was recently
598 demonstrated (Tosi et al. 2009, 2011). We demonstrated that all prolamins were able to
599 interact with each other in a yeast two-hybrid assay. However, in this yeast two-hybrid
600 system, protein interactions take place in a reducing environment, which is not totally
601 appropriate to permit the formation of intrachain disulphide bonds, which could lead to a
602 misfolding (Orsi et al. 2001). *In vivo* experiments should be assessed in order to confirm

these interactions in an appropriate environment context, in particular, to highlight the role of inter- and intrachain disulphide bonds in the trafficking of gliadins and glutenins. It would also be important to determine which part of the proteins contribute to the interaction in order to better understand the molecular mechanisms involved in the prolamin assembly formation.

To our knowledge, this is the first time that a LMW-G was fused to GFP and expressed in a plant model. Certainly due to the numerous repeated motifs and disulphide bonds along the sequences, prolamins, and particularly glutenins, are difficult to manipulate at the genetic level. We recently investigated the trafficking of high-molecular-weight glutenin fused to GFP in tobacco cell suspension BY-2, and we demonstrated its retention in ER and its ability to form PBLS (Saumonneau et al. 2011). The role of the repeated and cysteine-rich domains of γ-gliadin was explored using a similar strategy, leading to the conclusion that tobacco cells are a good model for studying atypical wheat prolamin trafficking with fluorescent protein fusions (Francin-Allami et al. 2011). Our study was focused on wheat LMW-glutenin and α-gliadin, which are two major types of wheat prolamins, and demonstrated their trafficking in tobacco cells. Taken together, these studies provide general information on the trafficking pathway of all wheat seed storage prolamins.

Supplementary material

Supplementary data are available at Plant Cell Reports online.

Supplementary Fig. S1. Nucleotide and amino acid sequences of α-gliadin used in this study.

Supplementary Fig. S2. Nucleotide and amino acid sequences of LMW-G used in this study.

Supplementary Movie S3. α-gliadin protein body-like structures (α-gliadin-GFP in green) moved throughout the cell along the ER network and are not co-localised with Golgi bodies (ST-mRFP$_1$ in red).

Supplementary Movie S4. Movie showing the absence of PBLS movement after Latrunculin B treatment.

Supplementary Fig. S5. No cell growth difference was detected between the non-transformed BY-2 and BY-2 expressing α-gliadin-GFP or LMW-G-GFP.

Acknowledgements

We are extremely grateful to Dominique Bozec (Nantes University, France) for culturing tobacco plants used for agrobacterium infiltration, Camille Alvarado (BIBS Platform, INRA Nantes, France) for technical assistance with TEM, Chris Hawes and Imogen Sparkes (Oxford Brookes University, UK), and to Lionel Gissot (Plateforme de Cytologie et d'Imagerie Végétale, INRA Versailles-Grignon, France) for providing some of the vectors and markers used in this study. BY-2 cells were kindly provided by Chris Hawes' laboratory, and anti-BiP antibodies were kindly provided by Ikuko Hara-Nishimura (Kyoto University, Japan).

References

Altschuler Y, Rosenberg N, Harel R, Galili G (1993) The N- and C-terminal regions regulate the transport of wheat γ-gliadin through the endoplasmic reticulum in Xenopus oocytes. Plant Cell 5:443-450

Banc A, Desbat B, Renard D, Popineau Y, Mangavel C, Navailles L (2009) Exploring the interactions of gliadins with model membranes: effect of confined geometry and interfaces. Biopolymers 91:610-622

Bietz JA, Huebner FR, Sanderson JE, Wall JS (1977) Wheat gliadin homology revealed through N-terminal amino-acid sequence-analysis. Cereal chemistry 54:1070 -1083

Coleman CE, Herman EM, Takasaki K, Larkins BA (1996) The maize gamma-zein sequesters alpha-zein and stabilizes its accumulation in protein bodies of transgenic tobacco endosperm. Plant Cell 8:2335-45

Conley AJ, Joensuu JJ, Menassa R and Brandle JE (2009) Induction of protein body formation in plant leaves by elastin-like polypeptide fusions. BMC Biol 7:48

Curtis MD, Grossniklaus U (2003) A gateway cloning vector set for high-throughput functional analysis of genes in planta. Plant Physiol 133:462-469

Foresti O, De Marchis F, De Virgilio M, Klein EM, Arcioni S, Bellucci M and Vitale A (2008) Protein domains involved in assembly in the endoplasmic reticulum promote vacuolar delivery when fused to secretory GFP, indicating a protein quality control pathway for degradation in the plant vacuole. Mol Plant 1:1067-76

Francin-Allami M, Saumonneau A, Lavenant L, Bouder A, Sparkes I, Hawes C, Popineau Y (2011) Dynamic trafficking of wheat γ-gliadin and of its structural domains in tobacco cells, studied with fluorescent protein fusions. J Exp Bot 62:4507-20

Galili G, Altschuler Y and Levanony H (1993) Assembly and transport of seed storage proteins. Trends Cell Biol 3:437-42

Geli MI, Torrent M, Ludevid D (1994) Two Structural Domains Mediate Two Sequential Events in γ-Zein Targeting: Protein Endoplasmic Reticulum Retention and Protein Body Formation. Plant Cell 6:1911-1922

Gomord V, Fitchette AC, Denmat LA, Michaud D, Faye L (1998) Production of foreign proteins in tobacco cell suspension culture. In Cunningham C, Porter AJR, eds. Methods in Molecular Biotechnology. Totowa, NJ, Humana Press 3:155-164

Hara-Nishimura II, Shimada T, Hatano K, Takeuchi Y, Nishimura M (1998) Transport of storage proteins to protein storage vacuoles is mediated by large precursor-accumulating vesicles. Plant Cell 10:825-836

Hatano K, Shimada T, Hiraiwa N, Nishimura M, Hara-Nishimura I (1997) A rapid increase in the level of binding protein (BiP) is accompanied by synthesis and degradation of storage proteins in pumpkin cotyledons. Plant Cell Physiol 38:344-51

Karimi M, De Meyer B and Hilson, P (2005) Modular cloning in plant cells. Trends Plant Sci 10:103–105

Kawagoe Y, Suzuki K, Tasaki M, Yasuda H, Akagi K, Katoh E, Nishizawa NK, Ogawa M, Takaiwa F (2005) The critical role of disulfide bond formation in protein sorting in the endosperm of rice. Plant Cell 17:1141-53

Kim CS, Woo Ym YM, Clore AM, Burnett RJ, Carneiro NP, Larkins BA (2002) Zein protein interactions, rather than the asymmetric distribution of zein mRNAs on endoplasmic reticulum membranes, influence protein body formation in maize endosperm. Plant Cell. 14:655-72

Laemmli UK (1970) Cleavage of structural proteins during the assembly of the head of bacteriophage T4. Nature 15:680-5

Levanony H, Rubin R, Altschuler Y and Galili G (1992) Evidence for a novel route of wheat storage proteins to vacuoles. J Cell Biol 119:1117-28

Li X, Wu Y, Zhang DZ, Gillikin JW, Boston RS, Franceschi VR, Okita TW (1993) Rice prolamine protein body biogenesis: a BiP-mediated process. Science 12:1054-1056

Llop-Tous I, Madurga S, Giralt E, Marzabal P, Torrent M, Ludevid MD (2010) Relevant elements of a maize gamma-zein domain involved in protein body biogenesis. J Biol Chem 285:35633-44

Lombardi A, Barbante A, Cristina PD, Rosiello D, Castellazzi CL, Sbano L, Masci S, Ceriotti A (2009) A relaxed specificity in interchain disulfide bond formation characterizes the assembly of a low-molecular-weight glutenin subunit in the endoplasmic reticulum. Plant Physiol 149:412-23

Loussert C, Popineau Y and Mangavel C (2008) Protein bodies ontogeny and localization of prolamin components in the developing endosperm of wheat caryopses. J. Cereal Sc 47:445-456

Marion J, Bach L, Bellec Y, Meyer C, Gissot L, Faure JD (2008) Systematic analysis of protein subcellular localization and interaction using high-throughput transient transformation of Arabidopsis seedlings. Plant J 56:169-79

Muench D.G, Wu Y, Zhang Y, Li X, Boston RS and Okita TW (1997) Molecular cloning, expression and subcellular localization of a BiP homolog from rice endosperm tissue. Plant Cell Physiol 38:404-12

Nagamine A, Matsusaka H, Ushijima T, Kawagoe Y, Ogawa M, Okita TW, Kumamaru T (2011) A role for the cysteine-rich 10 kDa prolamin in protein body I formation in rice. Plant Cell Physiol 52:1003-16

Parker ML and Hawes CR (1982) The Golgi-apparatus in developing endosperm of wheat (triticum aestivum L). Planta 154:277-283

Payne, PI (1987) Genetics of wheat storage proteins and the effect of allelic variation on bread-making quality. Annual Review of Plant physiology and Plant Molecular Biology 38:141-153

Pompa A, Vitale A (2006) Retention of a bean phaseolin/maize gamma-Zein fusion in the endoplasmic reticulum depends on disulfide bond formation. Plant Cell 18:2608-21

Randall JJ, Sutton DW, Hanson SF and Kemp JD (2005) BiP and zein binding domains within the delta zein protein. Planta 221:656-66

Rosenberg N, Shimoni Y, Altschuler Y, Levanony H, Volokita M, Galili G (1993) Wheat (Triticum aestivum L.) γ-Gliadin Accumulates in Dense Protein Bodies within the Endoplasmic Reticulum of Yeast. Plant Physiol 102:61-69

Reyes FC, Chung T, Holding D, Jung R, Vierstra R, Otegui MS (2011) Delivery of prolamins to the protein storage vacuole in maize aleurone cells. Plant Cell 2011:769-84

Rubin R, Levanony H and Galili G (1992) Evidence for the Presence of Two Different Types of Protein Bodies in Wheat Endosperm. Plant Physiol 99:718-724

Saito Y, Kishida K, Takata K, Takahashi H, Shimada T, Tanaka K, Morita S, Satoh S, Masumura T (2009) A green fluorescent protein fused to rice prolamin forms protein body-like structures in transgenic rice. J Exp Bot 60, 615-627

Saumonneau A, Rottier K, Conrad U, Popineau Y, Guéguen J, Francin-Allami M (2011) Expression of a new chimeric protein with a highly repeated sequence in tobacco cells. Plant Cell Rep 30:1289-302

Shewry PR, Tatham AS (1997) Disulphide bonds in wheat gluten proteins. Journal of Cereal Science 25:207-227

Shy G., Ehler L, Herman E and Galili G (2001) Expression patterns of genes encoding endomembrane proteins support a reduced function of the Golgi in wheat endosperm during the onset of storage protein deposition. J Exp Bot 52:2387-8

Shimoni Y, Galili G (1996) Intramolecular disulfide bonds between conserved cysteines in wheat gliadins control their deposition into protein bodies. J Biol Chem 271:18869-18874

Sparkes IA, Runions J, Kearns A, Hawes C (2006) Rapid, transient expression of fluorescent fusion proteins in tobacco plants and generation of stably transformed plants. Nat Protoc 1:2019-2025

Tamura K, Yamada K, Shimada T, Hara-Nishimura I (2004) Endoplasmic reticulum-resident proteins are constitutively transported to vacuoles for degradation. Plant J 39:393-402

Takemoto Y, Coughlan SJ, Okita TW, Satoh H, Ogawa M, Kumamaru T (2002) The rice mutant esp2 greatly accumulates the glutelin precursor and deletes the protein disulfide isomerase. Plant Physiol 128:1212-22

Tosi P, Parker M, Gritsch CS, Carzaniga R, Martin B and Shewry PR (2009) Trafficking of storage proteins in developing grain of wheat. J Exp Bot 60:979-91

Tosi P, Gritsch CS, He J, Shewry PR (2011) Distribution of gluten proteins in bread wheat (Triticum aestivum) grain. Ann Bot 108:23-35

Tsegaye Y, Richardson CG, Bravo JE, Mulcahy BJ, Lynch DV, Markham JE, JaworskiJG, Chen M, Cahoon EB, Dunn TM (2007) Arabidopsis mutants lacking long chain base phosphate lyase are fumonisin-sensitive and accumulate trihydroxy-18:1 long chain base phosphate. J Biol Chem 282:28195-206

Vitale A, Ceriotti A (2004) Protein quality control mechanisms and protein storage in the endoplasmic reticulum. A conflict of interests? Plant Physiol 136:3420-3426

Vitale A and Galili G (2001) The endomembrane system and the problem of protein sorting. Plant Physiol 125:115-8

Figure legends

Figure 1 Schematic representation of the α-gliadin and LMW-glutenin constructs used in the study. The Gateway recombination system was used to replace the CmR/*ccd*B vector cassette by the α-gliadin or LMW-glutenin cDNA, in order to construct C-terminal GFP/mRFP$_1$ fusions. All fusion constructs were placed under the control of the cauliflower mosaic virus double 35S promoter (2X35S) and the nopaline synthase terminator (T). Repeats (light grey box): N-terminal repeated sequence; C-rich (dark grey box): C-terminal cysteine-rich sequence; GFP/mRFP$_1$: green fluorescent protein/monomeric red fluorescent protein; black square: ER signal peptide; B1/B2/R1/R2: recombination sites; CmR/ccdB: Chloramphenicol resistance gene/*ccd*B gene; short lines: cysteine residues. The diagram is not drawn to scale.

Figure 2 Subcellular localisation of α-gliadin and LMW-glutenin fluorescent fusions in tobacco epidermal cells. Confocal microscope images showing GFP fusion proteins (green) expressed alone or coexpressed with mRFP$_1$ fusion markers (red) in tobacco leaf epidermal cells, 2-3 days after infiltration with Agrobacterium suspension cultures. Images of cells expressing α-gliadin-GFP (green) (a); α-gliadin-GFP (green) coexpressed with an mRFP$_1$-DPL1 ER marker (red) and merged image (b); α-gliadin-GFP (green) coexpressed with a Golgi marker, ST-mRFP$_1$ (red), and merged image (c); LMW-glutenin-GFP (green) (d); LMW-glutenin-GFP (green) coexpressed with an mRFP$_1$-DPL1 ER marker (red) and merged image (e); LMW-glutenin-GFP (green) coexpressed with a Golgi marker, ST-mRFP$_1$ (red) and merged image (f). Scale bars = 10 µm.

Figure 3 Classification of the transformed cells according to the protein body-like structures they contain.
Analysed cells were classified into three categories according to the density of prolamin protein body-like structures (PBLS) within the ER. The analysis was generated from confocal sections of transformed cells. The first category corresponds to cells containing a high PBLS density (more than 5 puncta/10 µm^2); the second category corresponds to cells containing a low PBLS density (less than 5 puncta/10 µm^2); and the third category corresponds to cells containing no apparent PBLS. The size of PBLS was taken into account in cell classification. Cells were provided from at least three individual transformation experiments in tobacco leaf

cells or BY-2 cells, transformed with each of the two constructs. A total of about 50 cells were examined for each transformation. The data were collected from transformed BY-2 cells comprised between 3 to 7 days of subculturing. The values are expressed as a percentage.

Figure 4 Immunoblotting from tobacco leaf epidermal cells expressing α-gliadin-GFP and LMW-glutenin-GFP. An immunoblot was performed with anti-GFP antibodies (a) or anti-BiP antibodies (b). (M): protein marker; (1): tobacco leaf expressing α-gliadin-GFP; (2): tobacco leaf expressing LMW-glutenin-GFP; (3): non-infiltrated tobacco leaf.

Figure 5 Electron micrographs of tobacco leaf epidermal cells expressing fused prolamins. Electron microscope images representing tobacco leaf epidermal cells 2-3 days after infiltration with Agrobacterium suspension cultures. Electron micrographs show areas in leaf epidermal cells expressing α-gliadin-GFP (a) or LMW-G-GFP (b) where PBLS (arrows) is demonstrated next to conventional rough ER. CW: cell wall; ER: endoplasmic reticulum; V: vacuole; C: cytosol. Scale bars = 0.5 µm.

Figure 6 Subcellular localisation of α-gliadin and LMW-glutenin fused to GFP in stable transgenic BY-2 cells. Subcellular localisation of α-gliadin-GFP or LMW-glutenin-GFP expressed in BY-2 cells 3, 5, 7 days or 10 days after subculturing. Scale bar = 20 µm.

Figure 7 Immunoblotting from tobacco cell suspension BY-2 expressing α-gliadin-GFP or LMW-glutenin-GFP. α-gliadin-GFP and GFP core, resulting from the same immunoblot, were revealed by an anti-GFP antibody from BY-2 cells expressing α-gliadin-GFP 2, 4 or 7 days after subculturing (a). LMW-glutenin-GFP and GFP core, resulting from the same immunoblot, were revealed by an anti-GFP antibody from BY-2 cells expressing LMW-glutenin-GFP 2, 4, 7 or 10 days after subculturing (b). BiP was revealed with an anti-BiP antibody (Hatano et al. 1997) (a, b). nt: non-transformed BY-2 cells. Immunoblotting performed with anti-BiP antibody from cells expressing α-gliadin-GFP 2, 4, 7 and 10 days after subculturing (c). Immunoblotting performed with anti-BiP antibody from 4-day-old BY-2 cells expressing homogenate subjected to differential centrifugation as previously described (Tamura et al. 2004) (d). P1: pellet fraction after a 1000 g centrifugation of the homogenate; P10: pellet fraction after a 10000 g centrifugation of the S1 supernatant; P100: pellet fraction

(microsomal fraction) after a 100 000 g centrifugation of the S10 supernatant; S100: 100 000 g supernatant (soluble vacuolar fraction).

Figure 8 α and γ-gliadins and LMW-glutenin fused to fluorescent protein locate to the same protein body-like structures in tobacco leaf epidermal cells. Confocal images of tobacco leaf epidermal cells transiently expressing LMW-glutenin-GFP (green), α-gliadin-mRFP$_1$ (red) and merge (a). Confocal images of tobacco leaf epidermal cells transiently expressing LMW-glutenin-GFP (green), γ-gliadin-mRFP$_1$ (red) and merge (b). Confocal images of tobacco leaf epidermal cells transiently expressing α-gliadin-GFP (green), γ-gliadin-mRFP$_1$ (red) and merge (c). Constructs were infiltrated and imaged 3 days after inoculation. Scale bars = 10 µm.

Figures

Figure 1

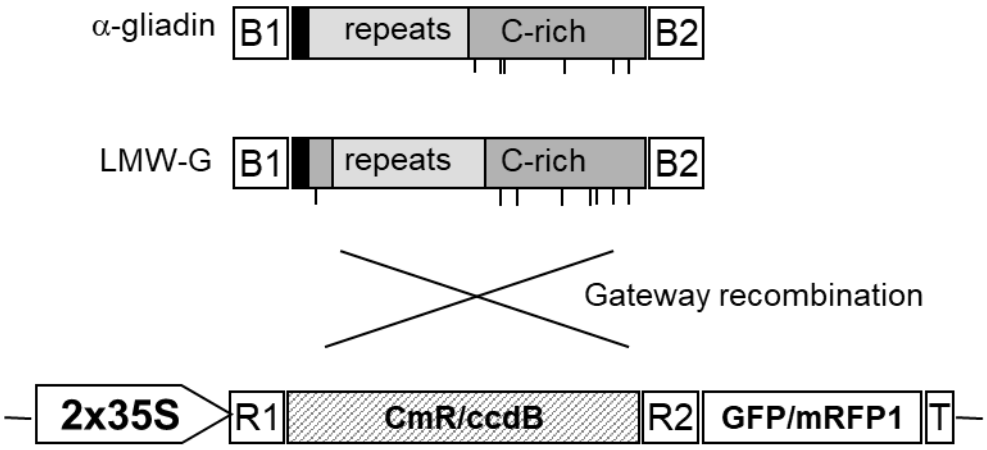

Figure 2

Figure 3

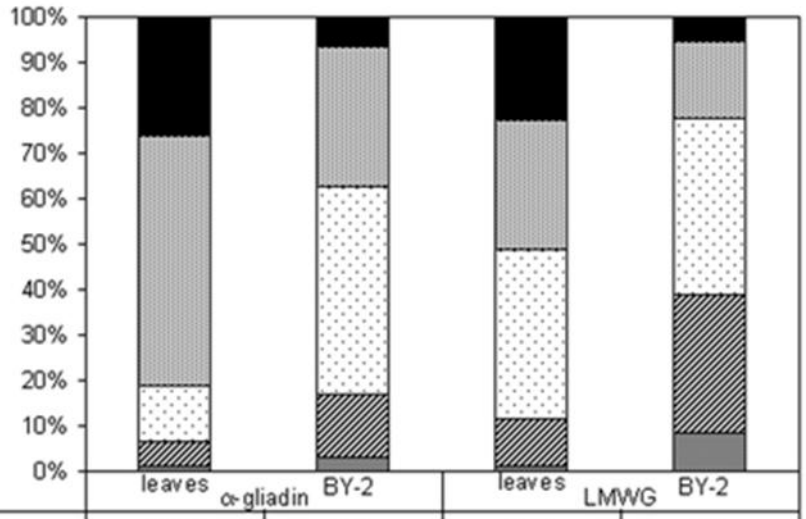

	α-gliadin leaves	α-gliadin BY-2	LMWG leaves	LMWG BY-2
high ER puncta density (presence of puncta>1µm)	26,2	6,4	22,7	5,5
high ER puncta density (puncta<1µm)	55	31	28,4	16,7
low ER puncta density (presence of puncta>1µm)	12,3	45,6	37,2	38,9
low ER puncta density (puncta<1µm)	5,3	13,8	10,4	30,5
without apparent ER puncta	1,2	3,2	1,3	8,4

Figure 4

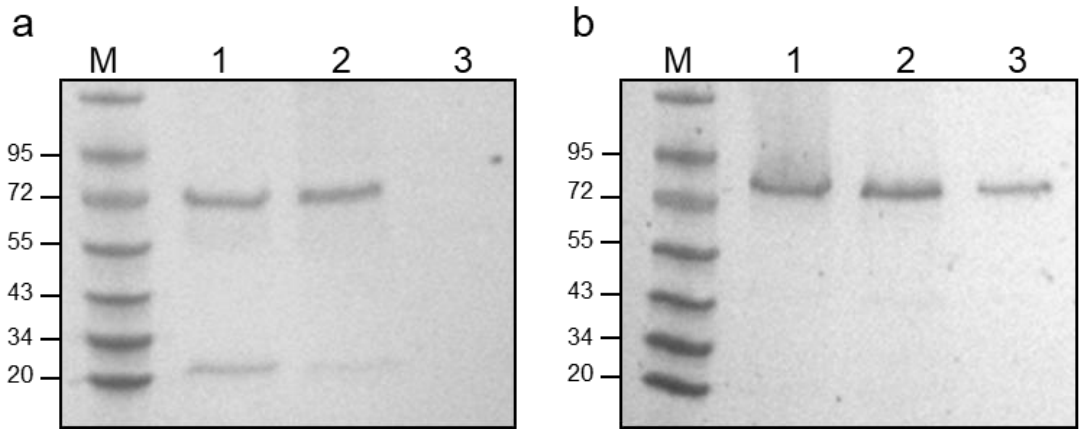

Figure 5

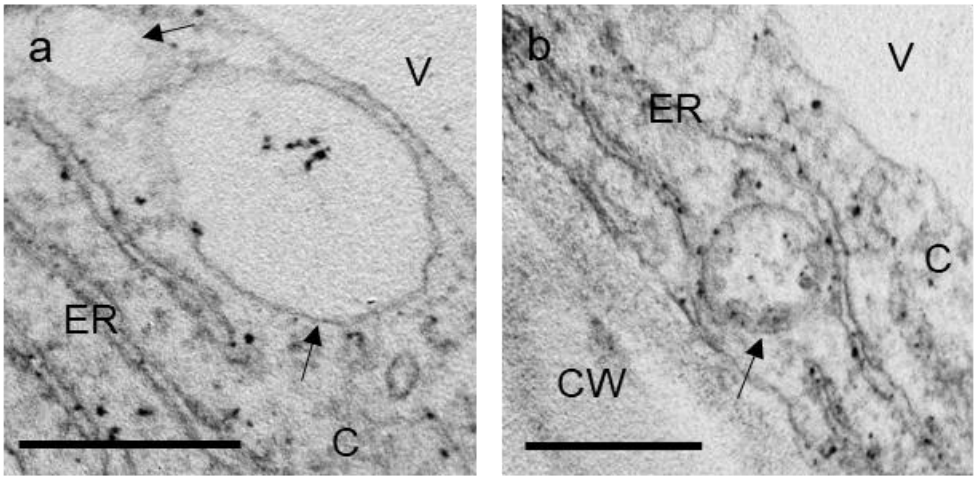

Figure 6

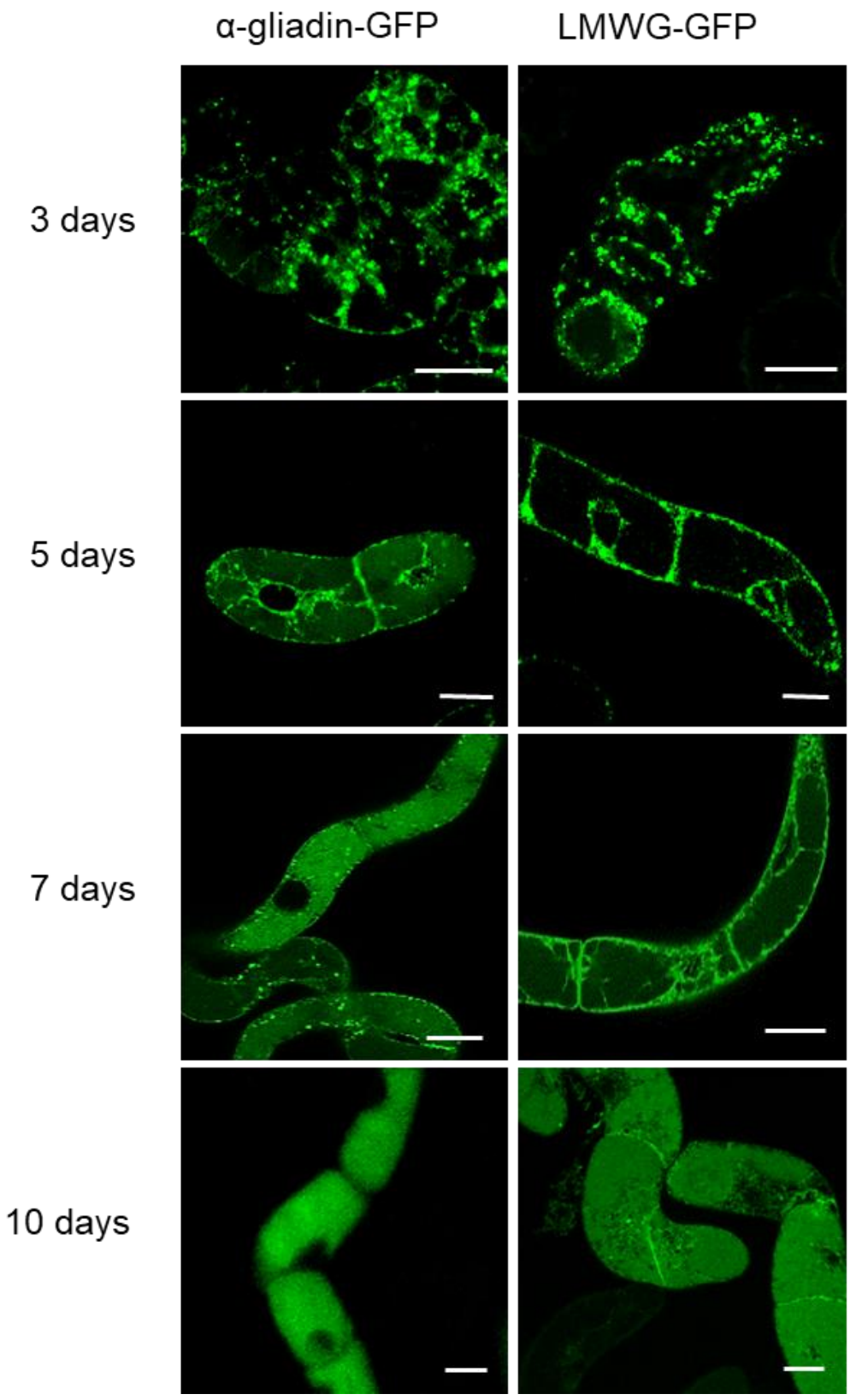

Figure 7

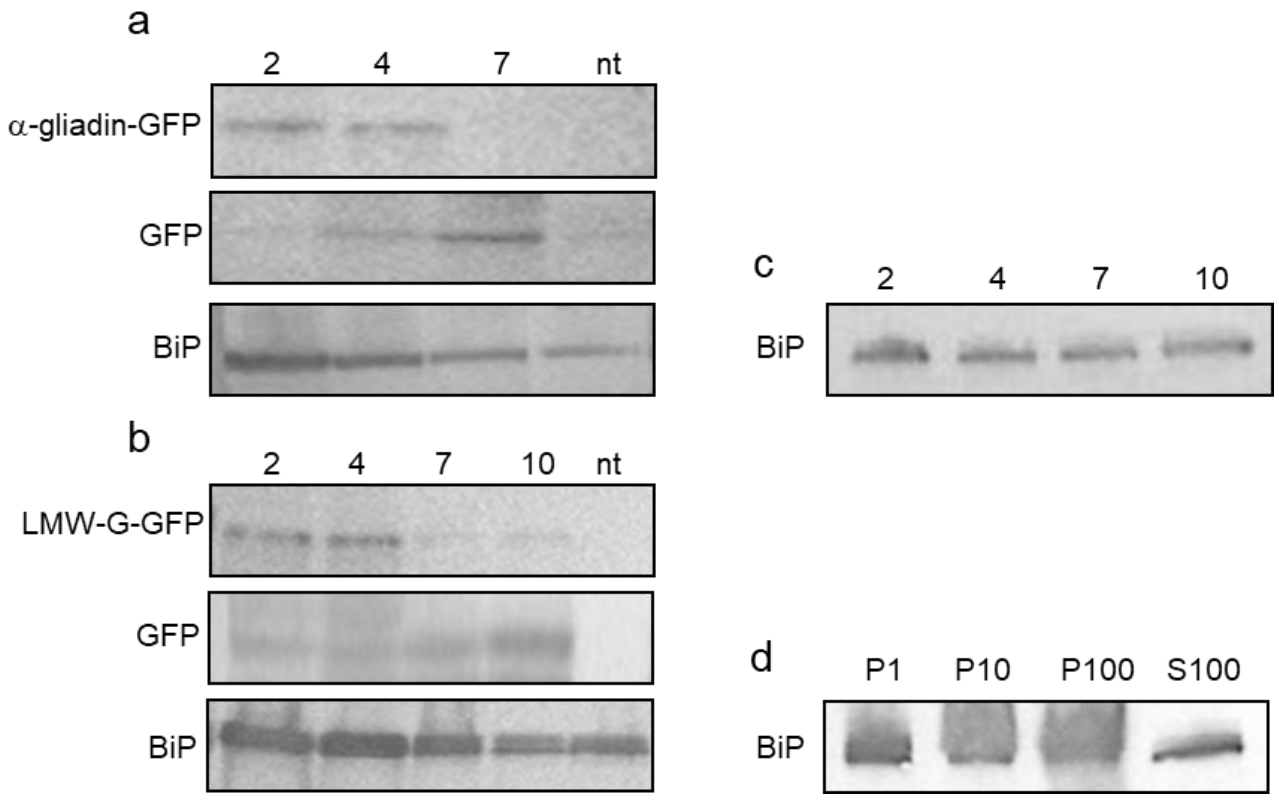
a
2
4
7
nt
α-gliadin-GFP
GFP
BiP
b
2
4
7
10
nt
LMW-G-GFP
GFP
BiP
c
2
4
7
10
BiP
d
P1
P10
P100
S100
BiP

Figure 8

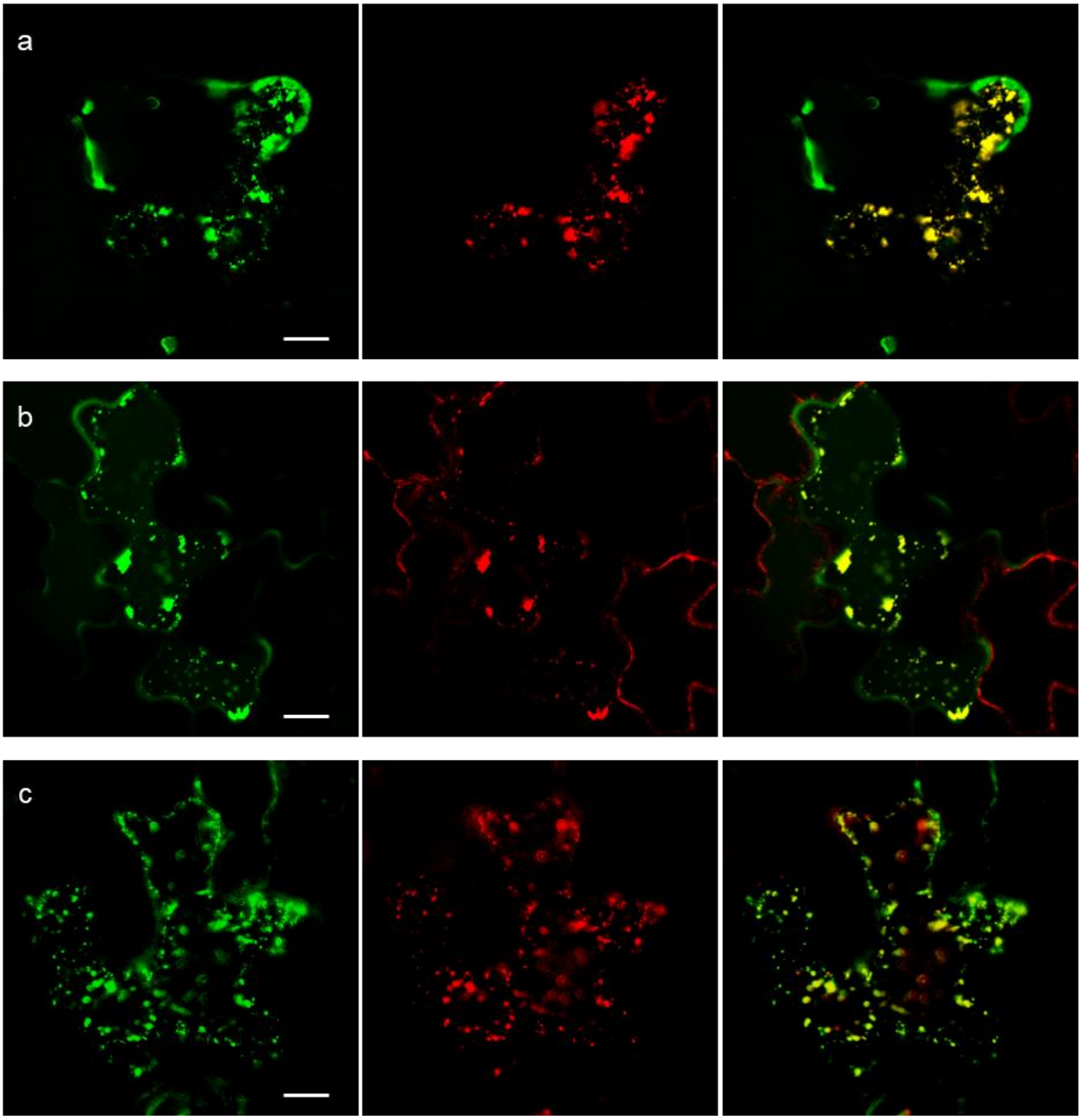

Tables

Table 1 Classification of transformed BY-2 cells according to their PBLS amount and vacuolar fluorescence during culture stages

Days	cells with high PBLS density (a)		cells with low PBLS density (b)		cells without PBLS (c)		vacuole fluorescence (d)	
of subculturing	α-gliadin	LMW-G	α-gliadin	LMW-G	α-gliadin	LMW-G	α-gliadin	LMW-G
3 d	85	63	14	25	1	12	0	0
5 d	15	13	77	72	8	15	73	2
7 d	2	5	62	43	36	52	98	56
10 d	0	0	0	9	100	91	100	91

Analysed cells were classified into three categories according to the density of PBLS at different stages of subculturing. The first category corresponds to cells with high PBLS density (more than 5 puncta/10 μm^2) (a); the second category corresponds to cells containing a low PBLS density (less than 5 puncta/10 μm^2) (b); and the third category corresponds to cells containing no apparent PBLS (c). In addition cells were also classified according to the vacuolar fluorescence they contain during subculturing stages (d). Cells provided from at least three individual transformation experiments in BY-2 cells transformed with each of the two constructs. A total of about 20 cells were examined for each transformation and culture stage. The values are expressed as a percentage.

Table 2 The interaction between α-gliadin, γ-gliadin and LMW-glutenin was performed using a yeast two-hybrid assay.

AD	BD	β-Gal
LMWG	α-gliadin	++
LMWG	γ-gliadin	+
LMWG	LMWG	+
LMWG	-	-
-	LMWG	-
α-gliadin	α-gliadin	++
α-gliadin	γ-gliadin	++
α-gliadin	LMWG	++
-	α-gliadin	-
α-gliadin	-	-

Column labelled “AD”: each prolamin was fused to the activator domain of GAL4 using the pACT prey vector; column labelled “DB”: each prolamin was fused to the binding domain of GAL4 using the pAS2.1 bait vector. Negative controls were performed by interacting constructs with empty prey or bait vectors (-). Results from β-galactosidase activity are summarised in the “β-Gal” column, and marked with +, ++, or – in accordance with the blue coloration intensity.